Lung Cancer: Targets and Therapy

ISSN: 1179-2728 (Online) Journal homepage: www.tandfonline.com/journals/dlct20

Elucidating the Role of FASN in Lung Cancer Stem Cells in Sensitive and Resistant EGFR-Mutated Non-Small Cell Lung Cancer Cells

Emma Polonio-Alcalá, Sira Ausellé-Bosch, Gerard Riesco-Llach, Pablo Novales, Lidia Feliu, Marta Planas, Joaquim Ciurana & Teresa Puig

To cite this article: Emma Polonio-Alcalá, Sira Ausellé-Bosch, Gerard Riesco-Llach, Pablo Novales, Lidia Feliu, Marta Planas, Joaquim Ciurana & Teresa Puig (2025) Elucidating the Role of FASN in Lung Cancer Stem Cells in Sensitive and Resistant EGFR-Mutated Non-Small Cell Lung Cancer Cells, Lung Cancer: Targets and Therapy, , 57-72, DOI: 10.2147/LCTT.S512936

To link to this article: https://doi.org/10.2147/LCTT.S512936

Published online: 27 May 2025.

Lung Cancer: Targets and Therapy

Dovepress
Taylor & Francis Group

Open Access Full Text Article

ORIGINAL RESEARCH

Elucidating the Role of FASN in Lung Cancer Stem Cells in Sensitive and Resistant EGFR-Mutated Non-Small Cell Lung Cancer Cells

Emma Polonio-Alcalá[1,2], Sira Ausellé-Bosch[1], Gerard Riesco-Llach[3], Pablo Novales[1], Lidia Feliu[3], Marta Planas[3], Joaquim Ciurana[2], Teresa Puig[1]

[1]New Therapeutic Targets Laboratory (Targetslab) – Oncology Unit, Department of Medical Sciences, University of Girona, Girona, Spain; [2]Product, Process, and Production Engineering Research Group (GREP), Department of Mechanical Engineering and Industrial Construction, University of Girona, Girona, Spain; [3]Laboratori d'Innovació en Processos i Productes de Síntesi Orgànica (LIPPSO), Department of Chemistry, University of Girona, Girona, Spain

Correspondence: Teresa Puig, Email teresa.puig@udg.edu

Introduction: Cancer stem cells (CSCs) drive tumor initiation, relapse, and metastasis. Our research team developed polycaprolactone electrospun (PCL-ES) scaffolds for enriching lung CSCs (LCSCs) since monolayer culture do not allow the study of this malignant population. The upregulation of fatty acid synthase (FASN) correlates with resistance to tyrosine kinase inhibitors (TKIs) targeting the epidermal growth factor receptor (EGFR), and its inhibition induces cytotoxicity in EGFR-mutated (EGFRm) non-small cell lung cancer (NSCLC) cells. Therefore, this study aims to elucidate the role of FASN and related signaling pathways in LCSCs cultured in PCL-ES scaffolds and to evaluate the effectiveness of FASN inhibitor G28, a synthetic derivative of (−)-epigallocatechin-3-gallate (EGCG), against this population.

Methods: EGFR-TKI-sensitive and -resistant cell modes were used. FASN expression and function were studied by RT-qPCR, Western blotting, and free fatty acid quantification, while related signaling pathways (EGFR, MAPK, AKT, and STAT3) were examined by Western blotting. The effects of G28 on LCSCs —including its impact on FASN and related signaling—were evaluated using the MTT assay and Western blotting.

Results: LCSCs cultured in PCL-ES scaffolds showed a significant FASN upregulation, supporting their proliferation and maintenance. Despite reduced EGFR activation in 3D-cultured cells, downstream signaling responses differed: PC9 cells exhibited higher levels of p-AKT, p-MAPK, and p-STAT3, while PC9-GR3 cells showed reduced p-MAPK and p-AKT, with no changes in p-STAT3. Regarding G28 treatment, it exhibited cytotoxic effects in both 2D- and 3D-cultured cells, suggesting potential efficacy in targeting both non-LCSCs and LCSCs. Furthermore, the treatment downregulated FASN and AKT, reducing or avoiding the proliferation of this malignant population.

Conclusion: Our results highlight the potential of G28 as a therapeutic option for targeting LCSCs in both sensitive and resistant EGFRm NSCLC cells, though additional studies are required to validate these results and assess their clinical applicability.

Keywords: lung cancer stem cells, FASN, EGCG synthetic derivative, NSCLC, 3D cell culture, AKT

Introduction

Lung cancer, as reported by the World Health Organization, is the most frequent cause of cancer-related fatalities globally for both men and women, representing 18.7% of all cancer-related deaths.[1] Non-small cell lung cancer (NSCLC) is the predominant subtype, with adenocarcinoma comprising nearly 40% of cases.

Epidermal growth factor receptor (EGFR) gene mutations are frequently observed in adenocarcinomas, occurring in about 38% of cases.[2] Mutations located within exon 19 (delE746_A750) and exon 21 (L858R point mutation) are the most prevalent.[3] The identification of these sensitizing mutations led to the generation of several EGFR tyrosine kinase inhibitors (EGFR-TKIs), for instance gefitinib and osimertinib.[4,5] Despite the initial favorable response, resistance to

Received: 20 January 2025
Accepted: 10 May 2025
Published: 27 May 2025

Graphical Abstract

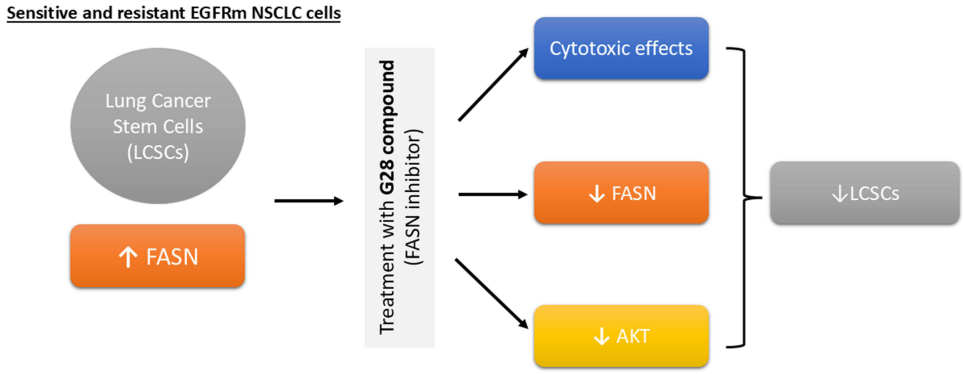

treatment inevitably develops in patients with lung cancer harboring EGFR mutations (EGFRm).[6,7] Several mechanisms of drug resistance have been described. These include secondary mutations (T790M, C797S), activation of alternative bypass or downstream pathways—for example, amplification of HER2 or MET, or mutations in PIK3CA, KRAS, or BRAF—overexpression of Axl, deletion of PTEN, and histological transformations.[8]

Cancer stem cells (CSCs), a minor subpopulation within tumors, possess unique characteristics such as resistance to traditional therapies, pluripotency, and self-renewal. These traits contribute to CSCs driving tumor initiation, progression, recurrence, and metastasis.[9] However, monolayer culture induces differentiation during cell expansion, resulting in the loss of stem-like properties.[10] To address this issue, previous studies conducted by our research group have demonstrated that polycaprolactone-electrospun (PCL-ES) scaffolds in three-dimensional (3D) cell culture effectively sustain the expansion of CSCs in breast and lung cancer.[11–13] These biocompatible systems provide a 3D architecture with nanofibers resembling the extracellular matrix, promoting cell attachment, proliferation, and phenotypic changes associated with malignancy.[13–15]

Dysregulation of cellular energy metabolism is fundamental to cancer cell growth and proliferation.[16] Consequently, FASN, the enzyme driving the *de novo* synthesis of fatty acids, mainly palmitate, is often overexpressed and/or hyperactivated in various types of cancers, including EGFRm NSCLC.[17] Specifically, EGFRm contributes to resistance to EGFR-TKIs by upregulating FASN expression.[18,19] As a result, we and others have shown that inhibiting FASN induces cytotoxicity and decreases the population of cancer stem-like cells in both sensitive and EGFR-TKI-resistant EGFRm lung cancer cells.[18–20] Although FASN upregulation has been involved in the maintenance and proliferation of CSCs in various malignancies,[21,22] its specific role in LCSCs, particularly in EGFRm NSCLC, remains poorly understood. Hence, this study aims to address this critical gap by investigating the contribution of FASN to LCSCs in EGFRm NSCLC, considering the clinical challenge in managing drug resistance and tumor relapse in these patients.

The (−)-epigallocatechin-3-gallate (EGCG) is a polyphenol known for its multiple properties, including anticancer, antimicrobial, antioxidant, and anti-inflammatory effects, among others.[23] The anticancer effects of EGCG are attributed to its ability to induce apoptosis, inhibit cell cycle, and modulate key signaling pathways, such as NF-κB, MAPK, PI3K/AKT, JAK/STAT, Wnt, and Notch. Additionally, EGCG suppresses angiogenesis, modulates invasion and metastasis, and inhibits tumor metabolism.[23] However, it exhibits low stability when exposed to physiological conditions.[24] To address this problem, the synthetic derivative compound G28 was developed, demonstrating cytotoxic effects on EGFRm NSCLC cells and 5.5-fold higher efficacy compared to EGCG. This compound also has the ability to inhibit the activity of FASN in both sensitive and resistant EGFRm NSCLC cells, while EGCG only in sensitive cells.[18] In contrast to other FASN inhibitors, G28 has demonstrated no induction of anorexia in animal models, indicating a more favorable safety profile. Furthermore, G28 did not cause tissue structural abnormalities, hepatic or renal dysfunction, nor did it alter hematological parameters.[25] Moreover, G28 has shown activity against CSCs in triple-negative breast cancer.[12,26]

Therefore, the main objectives of this study were to assess the role of FASN in lung CSCs (LCSCs) and evaluate the effectiveness of G28 against this subpopulation in both sensitive and EGFR-TKI-resistant EGFRm NSCLC cells.

Materials and Methods

Cell Models

The human lung adenocarcinoma cell line PC9 and its derivative, PC9-GR3, characterized by its resistance to gefitinib and osimertinib, were generously obtained from Dr. R. Rosell and Dr. M.A. Molina (Barcelona, Spain). Details regarding the resistance mechanisms of PC9-GR3 can be found elsewhere.[20] The cells were cultured under standard conditions using Roswell Park Memorial Institute (RPMI-1640) medium (Lonza, Basilea, Switzerland) supplemented with 10% fetal bovine serum (FBS) (HyClone, Logan, UT, USA) and 50 U/mL penicillin/streptomycin 10,000 U/mL (Lonza), maintained at 37 °C in a humidified environment with 5% CO2. Mycoplasma contamination was routinely monitored and prevented. The use of the cell lines was approved by the Ethics Committee for Investigation with Medicinal Products (CEIm) Girona.

Manufacturing of PCL Electrospun Scaffolds and 3D Cell Culture

To prepare a 15% (w/v) solution, polycaprolactone (PCL, Mn 80,000 g/mol, Sigma-Aldrich, St. Louis, MO, USA) was dissolved in acetone (min. ≥99.8%, PanReac AppliChem, Gatersleben, Germany) and stirred for 24 hours at 60 °C. Scaffolds were created using an electrospinning setup (Spraybase, Dublin, Ireland), where the solution was dispensed through a 20 mL syringe attached to an 18G stainless steel needle via a polytetrafluoroethylene tube with a 1 mm inner diameter. A 10 cm distance was maintained between the emitter and collector. The fabrication was conducted with the Syringe Pump Pro software (New Era Pump Systems, Farmingdale, NY, USA), applying a flow rate of 6 mL/h and a voltage of 7 kV to eject 5 mL of the polymer solution. The resulting electrospun meshes were trimmed into square dimensions of 2.56 cm^2 and 6.25 cm^2. Sterilization involved immersing the scaffolds in 70% ethanol (Labkem-Labbox Labware S.L., Barcelona, Spain) overnight, followed by two phosphate-buffered saline (PBS) (Lonza) rinses and UV light exposure for 30 minutes.

After sterilization, the scaffolds were placed in non-adherent cell culture plates (Sarstedt, Nümbrecht, Germany) and preconditioned in a supplemented medium at 37 °C in a humidified atmosphere with 5% CO2 for at least 30 minutes to promote cell adhesion. The cell suspension was prepared in 50 µL of medium for 12-well scaffolds and 75 µL for 6-well scaffolds, ensuring an appropriate seeding density. PC9 and PC9-GR3 cells were seeded onto the scaffolds as described in earlier studies.[20] As a control, monolayer cultures were established by seeding PC9 and PC9-GR3 cells onto adherent cell culture plates, ensuring equivalent cell confluency to those in the 3D scaffolds.

Quantitative Real-Time PCR Assessment

Both cell models were seeded in 2D and PCL scaffolds for periods of 3 and 6 days. After that, cells were harvested using 1× trypsin-EDTA (Dominique Dutscher, Bernolsheim, France) rinsed with PBS, and resuspended in 700 µL of Qiazol (Qiagen, Hilden, Germany). RNA extraction was performed using the GeneJET RNA Purification Kit (Thermo Fisher Scientific Inc., Waltham, MA, USA). The RNA was then quantified using the NanoDrop™ One Micro-volume UV–Vis spectrophotometer (Thermo Fisher Scientific) and reverse-transcribed to complementary DNA (cDNA) with the High Capacity cDNA Archive Kit (Applied Biosystems, Foster City, CA, USA). *FASN* and *GAPDH* gene expression were measured using specific primers (Supplementary Table 1) (Sigma-Aldrich) and qPCRBIO SyGreen Mix Lo-Rox (PCR Biosystems Inc., Wayne, PA, USA), with the assistance of the QuantStudio3 Real-Time PCR System machine (Thermo Fisher Scientific Inc). Relative gene expression was calculated with the $2^{\Delta CT}$ formula and normalized to *GAPDH* as the reference gene.

Protein Extraction and Western Blotting Assessment

Both cell models were seeded in 2D and PCL scaffolds for periods of 3 and 6 days. In case of G28 treatments, cells were seeded for 3 days and exposed to G28 for 48 hours. Compound G28 was synthesized by the LIPPSO research group (Girona, Spain).

After that, cells were collected using trypsin, rinsed with PBS, and suspended in lysis buffer (Cell Signaling Technology Inc., Danvers, MA, USA) with 100 µg/mL phenylmethylsulfonylfluoride (PMFS, Sigma-Aldrich). The cell lysates were obtained by vortexing for 20 seconds every 5 minutes for a total of 30 minutes at 4 °C. Protein concentration of each sample was determined using the DC Protein Assay (Bio-Rad, Hercules, CA, USA), referencing a bovine serum albumin (BSA, ≥98.0%, Sigma-Aldrich) standard curve. Equal amounts of protein were denatured in reducing agent and lithium dodecyl sulfate buffers (Invitrogen, Carlsbad, CA, USA) by heating at 70 °C for 10 minutes. SDS-polyacrylamide gel electrophoresis (Bio-Rad) was performed to separate the proteins, which were then transferred onto nitrocellulose membranes (Thermo Fisher Scientific Inc). Membranes were blocked for 3 hours at room temperature in blocking buffer [5% BSA (PanReac AppliChem) in tris-buffered saline (TBS, PanReac AppliChem) 0.05% Tween (PanReac AppliChem)] and incubated overnight at 4°C with the appropriate primary antibody (Supplementary Table 1) (Cell Signaling Technology and Abcam, Cambridge, UK), diluted in blocking buffer. Subsequently, the membranes were incubated for 1 hour and 30 minutes at room temperature with specific horseradish peroxidase-conjugated secondary antibodies. Protein detection was carried out using the Bio-Rad ChemiDoc™ MP Imaging System (Bio-Rad) and Clarity™ Western ECL Substrate (Bio-Rad) or West Femto Maximum Sensitivity Substrate (Thermo Fisher Scientific Inc).

Free Fatty Acid (FFA) Quantification Assay

PC9 and PC9-GR3 cells were seeded in 2D and PCL scaffolds for 3 and 6 days. After that, 1,000,000 cells were collected with trypsin, rinsed with PBS, and suspended in 200 µL of chloroform-1% Triton X-100 (Labkem-Labbox Labware S.L). The protocol from Free Fatty Acid Quantitation Kit (Sigma-Aldrich) was employed to extract fatty acids. The organic phase from the mixtures was separated and dried at 50 °C, followed by vacuum drying for 30 minutes to eliminate residual chloroform. Subsequently, the resulting fatty acids were resuspended in Fatty Acid Assay Buffer, and a standard curve of palmitic acid was prepared. The samples were mixed with ACS Reagent and Master Reaction Mix and incubated for 30 minutes at 37 °C with each agent. The absorbance was measured at 570 nm and the results were calculated to determine the concentration of fatty acids.

Cell Viability Assay

Both cell models were seeded in 2D and PCL scaffolds for a period of 3 days. After that, cells were exposed to different concentrations of G28 for 48 hours. The 3D structures were rinsed twice with PBS and relocated into clean wells to guarantee that exclusively live and adhered cells were considered for this assessment. 3-(4,5–dimethyl-2–thiazolyl)-2,5–diphenyl-2 H-tetrazolium bromide (MTT, Sigma-Aldrich) assay was performed to assess cell viability, following previously established protocols.[27]

Data Analysis

The IBM SPSS software (Version 25.0; SPSS Inc., Chicago, IL, USA) was employed to conduct the pertinent analyses. Experiments were conducted in triplicate or more, and results are expressed as the mean ± standard error of the mean (SE). Parametric data were analyzed using the Student's *t*-test or one-way analysis of variance (ANOVA), followed by Tamhane's T2 or Bonferroni post hoc tests, as appropriate. For non-parametric data, the Mann-Whitney *U*-test or Kruskal–Wallis test was applied, depending on the number of groups being compared. Statistical significance was set at $p < 0.050$, with results visualized as follows: $p < 0.050$ (*), $p < 0.010$ (**), and $p < 0.001$ (***).

Results

FASN Activity and Expression in LCSCs Cultured in PCL-ES Scaffolds

Gene and protein expression of FASN and its enzymatic activity were determined in both 2D- and 3D-cultured cells using RT-qPCR, immunoblotting, and FFA quantification assay, respectively. These analyses aimed to elucidate the role of FASN in PC9 and PC9-GR3 cells cultured in PCL-ES scaffolds, which enable the expansion of the LCSC niche (Figure 1).

LCSCs seeded in PCL-ES scaffolds for 3 days exhibited elevated *FASN* mRNA and protein levels and a higher quantity of FFAs. Analysis of *FASN* mRNA levels revealed a significant rise at both 3 and 6 days in the 3D-cultured cells compared to cells seeded in monolayer (PC9, 3 days: p=0.004, 6 days: p= 0.000046; PC9-GR3, 3 days: p=0.029, 6 days: p=0.028). Similarly, 3D-cultured PC9 cells demonstrated a significant upregulation of FASN protein levels at both times assessed (3 days: p=0.006; 6 days: p=0.001) compared to 2D. However, in PC9-GR3 cells, although a slight increase of FASN protein expression was observed at 3 days, its levels were comparable between 2D- and 3D-cultured cells after 6 days. Regarding the quantification of FFAs, there was a tendency for elevated levels in both cell models at 3 days, while the values were similar between 2D and 3D culture platforms at 6 days. Hence, these findings suggest FASN activity was enhanced in both PC9 and PC9-GR3 cells cultured in PCL-ES scaffolds for the initial 3 days.

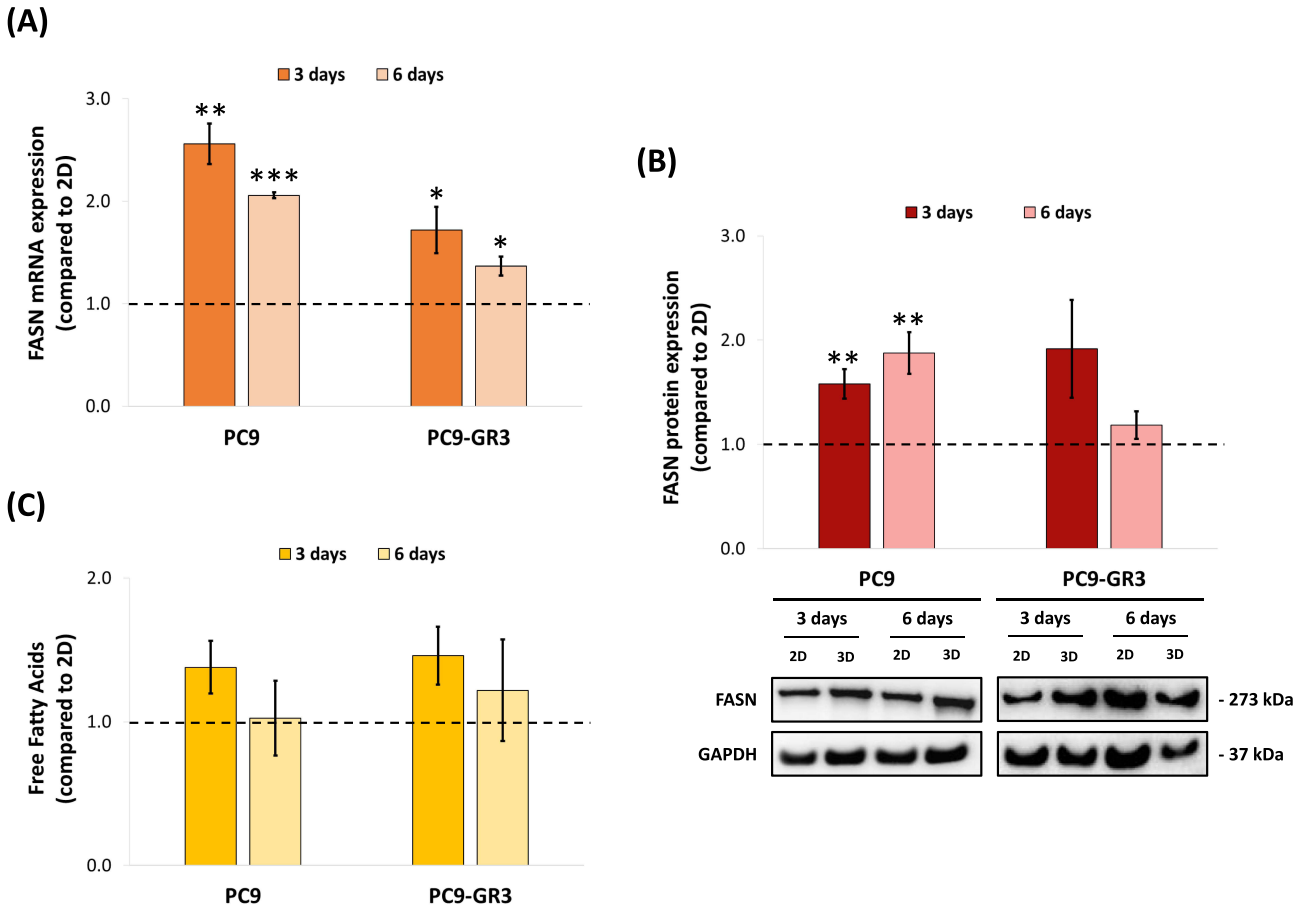

Figure 1 The role of FASN in LCSCs from both sensitive (PC9) and gefitinib- and osimertinib-resistant (PC9-GR3) cell models cultured in PCL-ES scaffolds. (**A**) *FASN* mRNA levels. mRNA expression was normalized against *GAPDH* gene. (**B**) FASN protein expression. GAPDH was used as a loading control. (**C**) Free fatty acid quantification. The concentration of free fatty acids was quantified using a standard curve of palmitic acid. In each analysis, cells were cultured in 2D and PCL-ES scaffolds for 3 and 6 days. The 3D cell culture condition was compared to monolayer culture, which was normalized to the value of 1 (represented by the dotted line) and expressed as fold change. The results are presented as mean ± SEM from a minimum of three independent experiments. The symbol * indicates statistically significant differences compared to 2D Ctrl (* $p < 0.05$, ** $p < 0.01$, and *** $p < 0.001$).

https://doi.org/10.2147/LCTT.S512936

EGFR, AKT, MAPK, and STAT3 Expression of LCSCs Cultured in PCL-ES Scaffolds

EGFR, AKT, MAPK, and STAT3 protein expression were assessed by Western blotting in cells cultured in both monolayer and 3D. The objective of this experiment was to investigate the involvement of these signaling pathways in PC9 and PC9-GR3 cells cultured in PCL-ES scaffolds (Figure 2).

The EGFR receptor was downregulated both in sensitive and resistant cells cultured in 3D. Specifically, a notable decrease in total EGFR levels was evident at 3 days (p=0.013) and 6 days (p=0.001) in sensitive cells compared to 2D-cultured cells, while resistant cells exhibited this reduction only at 6 days (p=0.001). Additionally, regarding p-EGFR expression, diminished levels were observed at 6 days (p=0.012) in 3D-cultured sensitive cells and both at 3 days (p=0.001) and 6 days (p=0.064) in 3D-cultured resistant cells.

PC9 cells cultured in 3D exhibited activation of MAPK and STAT3 proteins at 3 and 6 days compared to 2D-cultured cells (p-MAPK 3d: p=0.055; p-STAT3 3d: p=0.070; p-STAT3 6d: p=0.002). Moreover, total MAPK expression was upregulated significantly at 3 and 6 days (p=0.007 and p=0.015, respectively). In contrast, there was a tendency for total STAT3 levels to decrease at 3 days (p=0.085). Regarding AKT, total expression tended to increase after 3 days of 3D culture (p=0.095), with no concurrent change in its activation. However, at 6 days of culture, total expression levels were similar to those of monolayer culture, while its activation levels increased. Notably, these differences observed were not statistically significant.

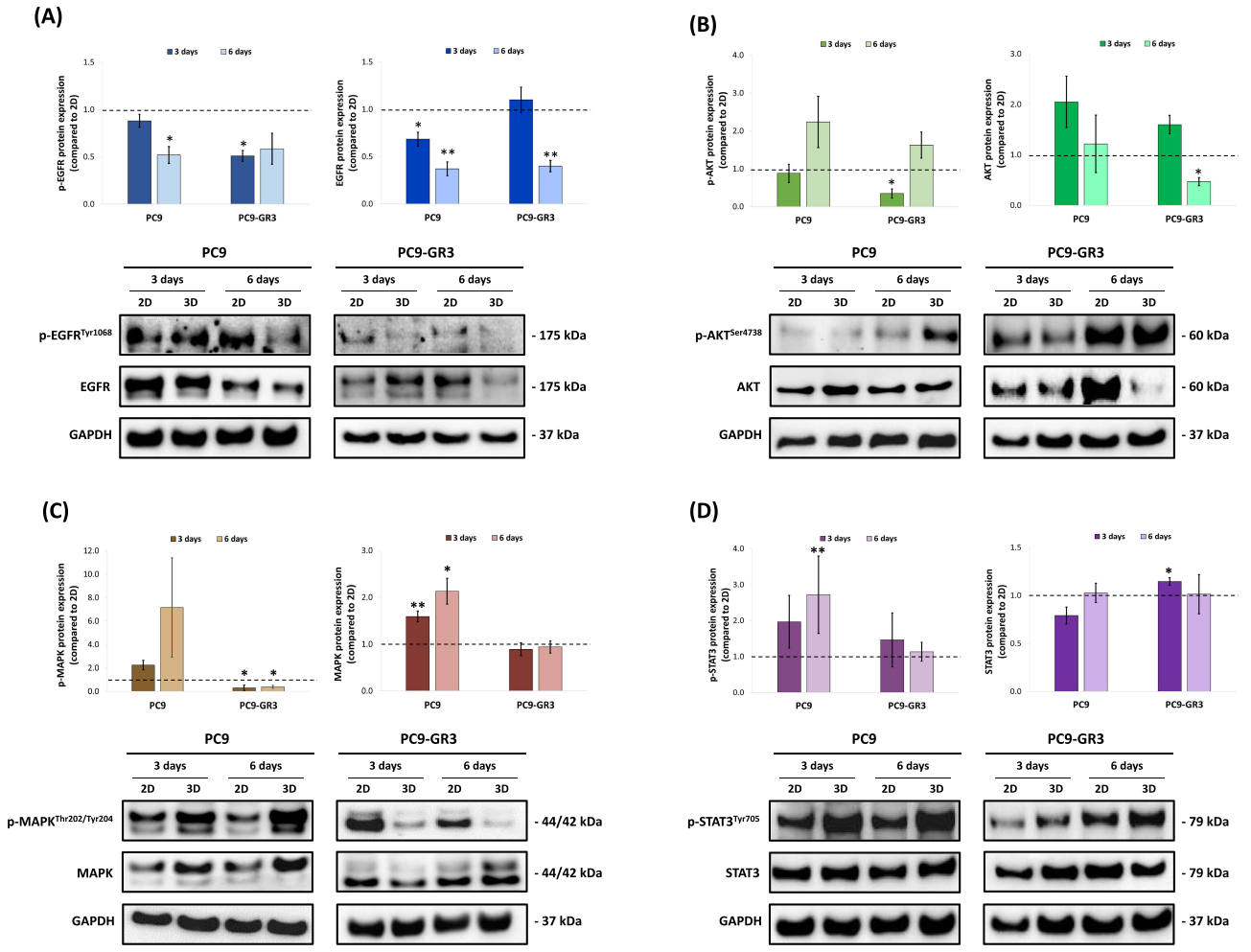

Figure 2 Analysis of phosphorylated and total protein expression of (**A**) EGFR, (**B**) AKT, (**C**) MAPK, and (**D**) STAT3 in both sensitive (PC9) and gefitinib- and osimertinib-resistant (PC9-GR3) cells cultured in 2D and PCL-ES scaffold for 3 and 6 days. GAPDH was used as a loading control. The 3D cell culture condition was compared to monolayer culture, which was normalized to the value of 1 (represented by the dotted line) and expressed as fold change. A representative Western blot image for each cell culture condition is presented. The results are presented as mean ± SEM from a minimum of three independent experiments. The symbol * indicates statistically significant differences compared to 2D Ctrl (* $p < 0.05$ and ** $p < 0.01$).

https://doi.org/10.2147/LCTT.S512936

The expression of the proteins analyzed in PC9-GR3 cells cultured in 3D exhibited remarkable differences compared to the PC9 cell model. On one hand, no variations were observed in the total levels of MAPK compared to 2D-cultured cells. Total AKT expression was significantly decreased (p=0.022) at 6 days, whereas total STAT3 levels showed a slight yet significantly increase (p=0.020) at 3 days. On the other hand, there was a significant decline in p-MAPK at both 3 and 6 days (p=0.029 and p=0.020, respectively), compared to monolayer culture. Notably, p-AKT expression significantly reduced only at 3 days (p=0.033). No changes were displayed in p-STAT3 expression.

G28 Treatment Against LCSCs Cultured in PCL-ES Scaffolds

Following the elucidation of the role of FASN and the signaling pathways of EGFR, AKT, MAPK, and STAT3 in 3D-cultured cells, the therapeutic potential of G28 was evaluated on sensitive and resistant cell models cultured in PCL-ES scaffolds. Hence, cell viability was analyzed in PC9 and PC9-GR3 cells seeded in 2D and 3D culture for 3 days, and subsequently treated with G28 for an additional 48 hours (Figure 3A).

The sensitive cell model, whether cultured in monolayer or PCL-ES scaffolds, showed a similar response to G28 treatment, with an IC_{50} of 53.9 µM in 2D and 57.4 µM in 3D (p=0.777). In contrast, the resistant cell model exhibited a lower IC_{50} value of 31.2 µM when seeded in 2D compared to 3D-cultured cells, 65.8 µM (p=0.087).

Interestingly, both PC9 and PC9-GR3 cells, regardless of cell culture system, demonstrated similar cell viability across all G28 doses, except for 30 µM, in which the cell response significantly differed between cells cultured in 2D and 3D (PC9: p=0.039; PC9-GR3: p=0.004).

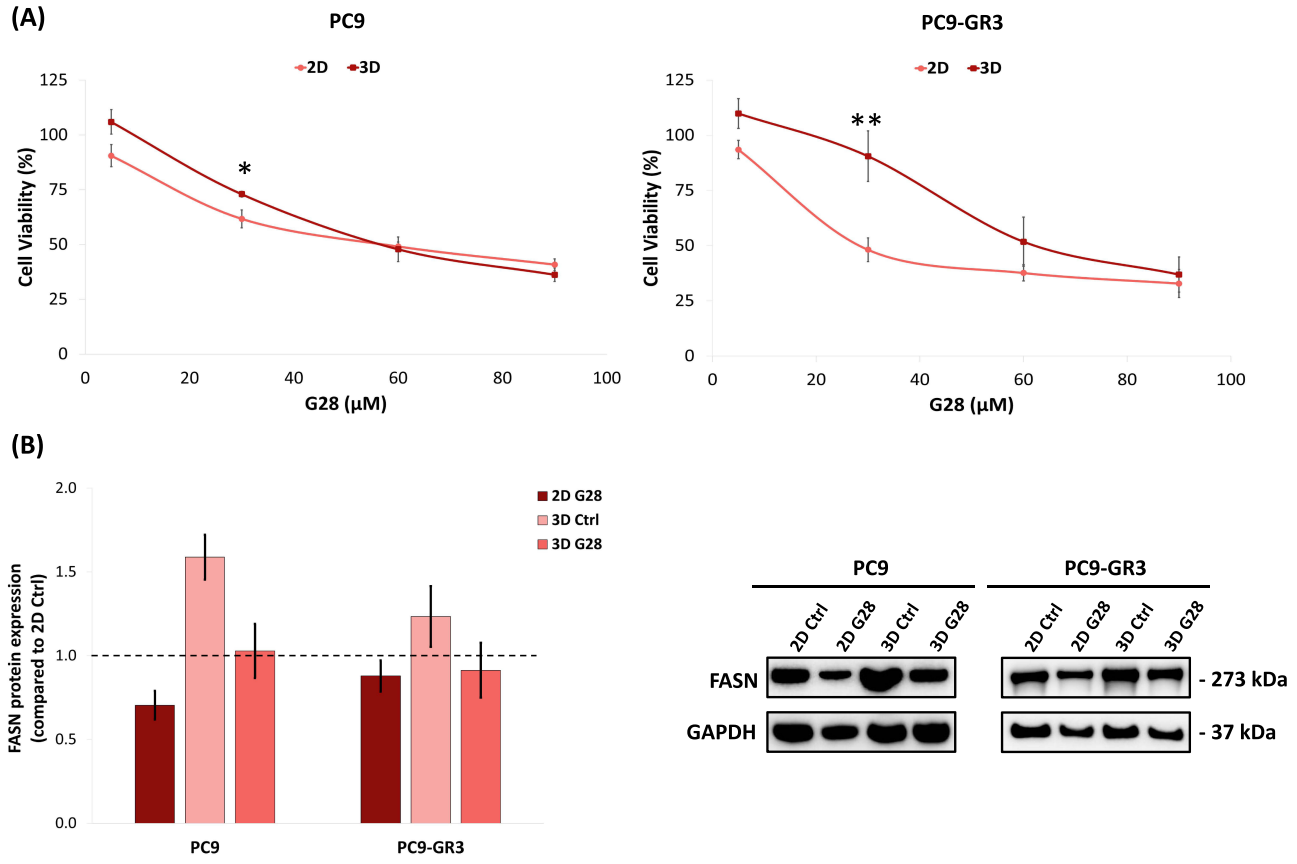

Figure 3 (**A**) Cell viability of both sensitive (PC9) and gefitinib- and osimertinib-resistant (PC9-GR3) cells cultured in 2D and PCL-ES scaffolds for 3 days and then treated with G28 for 48 hours. Results are expressed as the percentage of surviving cells (mean ± SEM) compared to untreated cells from at least three independent experiments. (**B**) FASN protein expression PC9 and PC9-GR3 cell models cultured in 2D and PCL-ES scaffolds for 3 days and then treated with G28 for 48 hours. GAPDH was used as a loading control. All cell culture conditions were compared to 2D, which was normalized to the value of 1 (represented by the dotted line) and expressed as fold change. A representative Western blot image for each cell culture condition is presented. The results are presented as mean ± SEM from a minimum of three independent experiments. The symbol * indicates statistically significant differences compared to 2D Ctrl (* $p < 0.05$ and ** $p < 0.01$).

https://doi.org/10.2147/LCTT.S512936

In addition, FASN protein expression was determined after the treatment with G28 (Figure 3B). As previously observed, sensitive and resistant cells cultured in PCL-ES scaffolds demonstrated an upregulation of FASN expression, more evident in PC9 cells. The treatment with G28 reduced FASN protein expression in 2D- and 3D-cultured cells in PC9 cells, while in PC9-GR3 cells, the treatment reduced slightly its expression. Notably, FASN expression in 3D culture after G28 treatment was decreased to levels comparable to those showed in control monolayer culture.

Molecular Effects of G28 Treatment on LCSC Biomarkers of LCSCs Cultured in PCL-ES Scaffolds

LCSC biomarkers, including CD166, E-cadherin, and Sox2, were assessed by means of Western blotting in PC9 and PC9-GR3 cells cultured in both 2D and 3D conditions for 3 days, followed by the administration of G28 for an additional 48 hours. This analysis was conducted to discern the alterations in LCSC biomarkers caused by G28 (Figure 4).

Treatment with G28 in monolayer-seeded cells induced a slight reduction in CD166 expression in both cell models, along with a decrease in SOX2 expression and an upregulation of E-cadherin levels in PC9 cells.

Regarding LCSC expansion using PCL-ES scaffolds, the sensitive model showed increased levels of CD166 and p-SOX2 alongside diminished E-cadherin expression, while the resistant model exhibited solely a decline in E-cadherin levels. The treatment with G28 resulted in a reduction in CD166 and p-SOX2 levels in PC9 cells seeded in 3D, with no variations in other analyzed LCSC markers. Regarding PC9-GR3 cells, no changes were observed in any LCSC marker after the treatment with G28 in 3D-cultured cells.

Molecular Effects of G28 Treatment on EGFR, AKT, MAPK, and STAT3 of LCSCs Cultured in PCL-ES Scaffolds

EGFR, AKT, MAPK, and STAT3 protein expression were analyzed by Western blotting in cells cultured in both monolayer and PCL-ES scaffolds for 3 days, and then treated with G28 for an additional 48 hours. This experiment aimed to investigate the changes induced by G28 in these signaling pathways (Figure 5).

In PC9 cells, the treatment with G28 significantly reduced STAT3 activation in both 2D- ($p= 0.000002$) and 3D-cultured cells ($p=0.000002$ compared to 3D Ctrl; $p= 0.000007$ compared to 2D Ctrl). There was also a tendency for decreased p-AKT levels observed only in 3D-seeded cells ($p=0.075$ compared to 3D Ctrl), while a significant decrease in total AKT was noticeable in both 2D ($p=0.040$) and 3D ($p=0.032$ compared to 2D Ctrl; $p=0.044$ compared to 3D Ctrl) cultures. Although a slight reduction was displayed in p-MAPK and total MAPK expression in 2D-cultured cells, no alterations were showed in cells cultured on PCL-ES scaffolds. No changes were neither observed in the expression of p-EGFR, nor in total STAT3. Interestingly, cells treated with G28 exhibited a slight increase in total EGFR levels.

In PC9-GR3 cells, the treatment with G28 significantly elevated EGFR activation in both 2D- ($p= 0.006$) and 3D-cultured cells ($p=0.041$). Moreover, a reduction in p-AKT and p-MAPK ($p=0.044$ compared to 2D Ctrl) levels was noted in cells seeded on PCL-ES scaffolds. A significant increase in total EGFR expression in 2D-seeded cells ($p=0.014$) and a slight decrease in total STAT3 levels were also observed in both culture systems. No variations were displayed in total AKT and MAPK, nor in p-STAT3 expression.

Discussion

The research about CSCs is essential since they are responsible for tumor initiation, relapse, and metastasis.[9] However, this malignant subpopulation cannot be studied using traditional cell culture methods.[10] To bridge this gap, our research group developed PCL-ES scaffolds for the expansion of LCSCs, enabling their investigation in vitro.[13] Additionally, the upregulation of FASN has been linked to resistance to EGFR-TKIs and inhibition of this enzyme exhibited a cytotoxic effect in both sensitive and EGFR-TKI-resistant EGFRm NSCLC cells and cancer stem-like cells.[18–20] In previous studies, we demonstrated the efficacy of the compound G28, a synthetic derivative of EGCG, in inhibiting FASN activity and inducing cytotoxic effect in both sensitive and EGFR-TKI-resistant EGFRm NSCLC cells,[18] and in targeting CSCs in triple-negative breast cancer.[12,26] Therefore, this study aims to elucidate the involvement of FASN and its associated

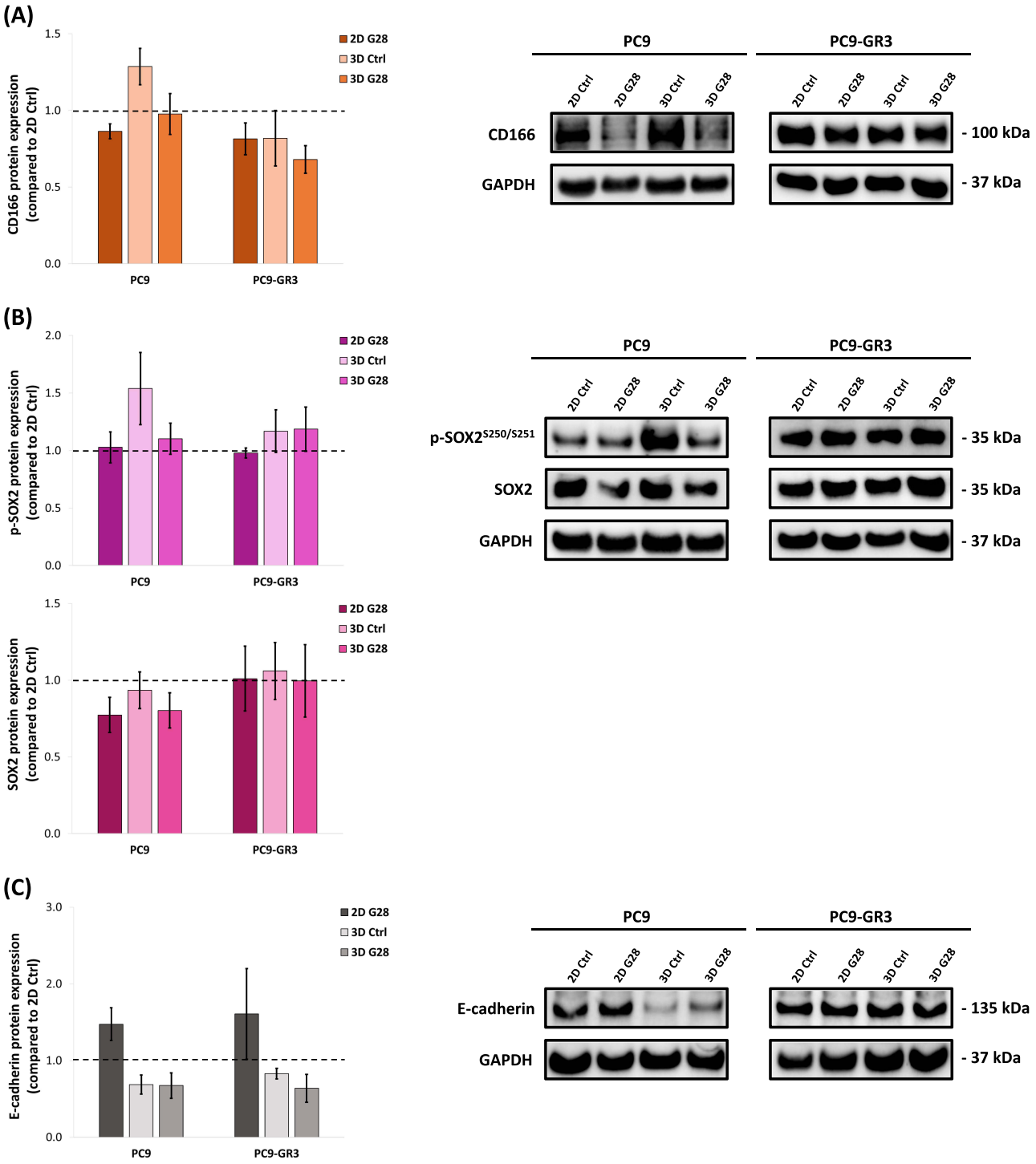

Figure 4 Analysis of (**A**) CD166, (**B**) phosphorylated and total SOX2, and (**C**) E-cadherin protein expression in both sensitive (PC9) and gefitinib- and osimertinib-resistant (PC9-GR3) cells cultured in 2D and PCL-ES scaffolds for 3 days and then treated with G28 for 48 hours. GAPDH was used as a loading control. All cell culture conditions were compared to 2D, which was normalized to the value of 1 (represented by the dotted line) and expressed as fold change. A representative Western blot image for each cell culture condition is presented. The results are presented as mean ± SEM from a minimum of three independent experiments.

signaling pathways in the LCSC niche and to evaluate the effectiveness of G28 in eradicating LCSC subpopulation in both sensitive and EGFR-TKI-resistant EGFRm NSCLC cells.

To achieve the first objective, gene and protein expression of FASN, along with its enzymatic activity, were initially determined in LCSCs cultured in PCL-ES scaffolds (Figure 1). A significant upregulation of FASN expression, as well as

https://doi.org/10.2147/LCTT.S512936

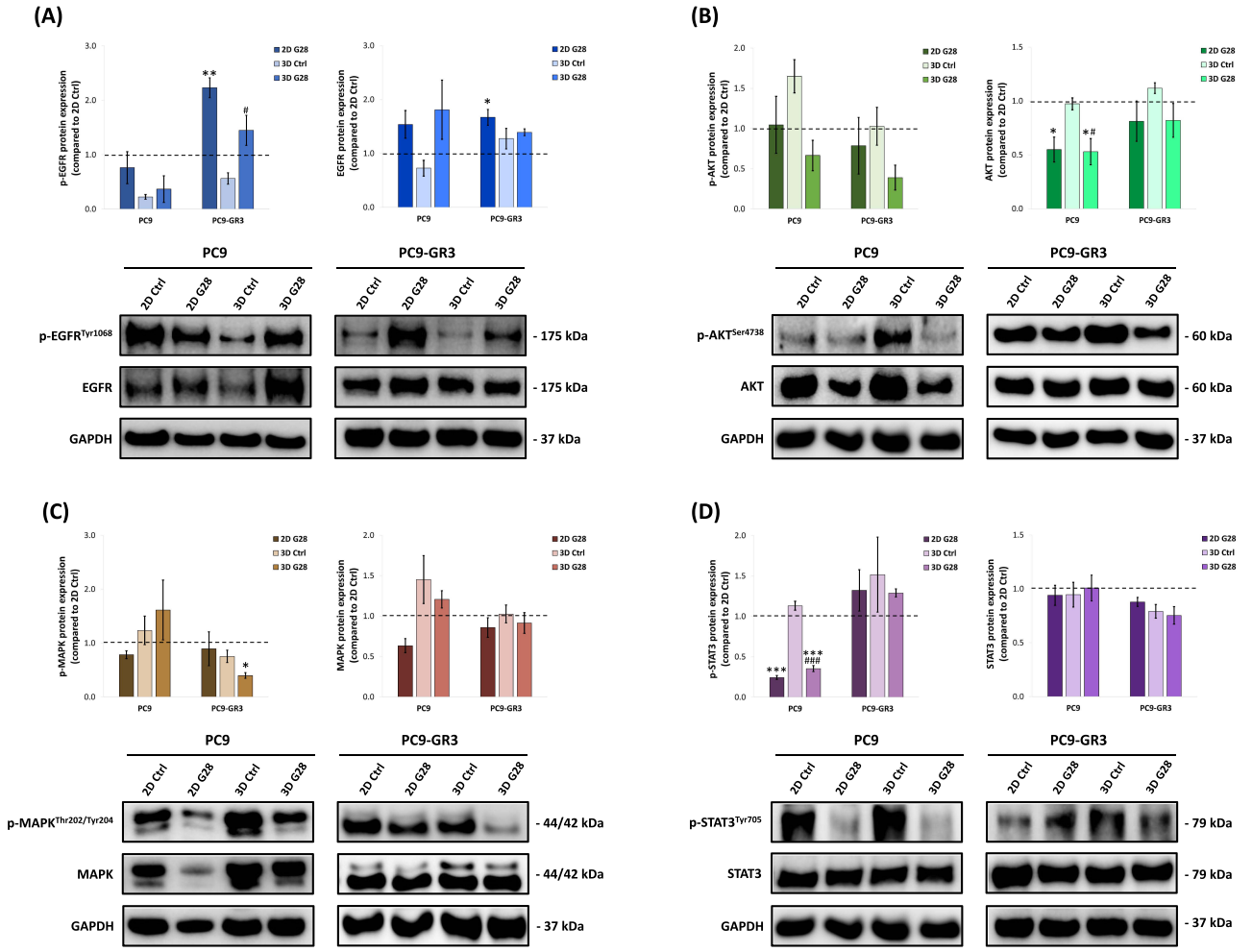

Figure 5 Analysis of phosphorylated and total protein expression of (**A**) EGFR, (**B**) AKT, (**C**) MAPK, and (**D**) STAT3 in both sensitive (PC9) and gefitinib- and osimertinib-resistant (PC9-GR3) cells cultured in 2D and PCL-ES scaffolds for 3 days and then treated with G28 for 48 hours. GAPDH was used as a loading control. All cell culture conditions were compared to 2D, which was normalized to the value of 1 (represented by the dotted line) and expressed as fold change. A representative Western blot image for each cell culture condition is presented. The results are presented as mean ± SEM from a minimum of three independent experiments. The symbol * indicates statistically significant differences compared to 2D Ctrl (* $p < 0.05$, ** $p < 0.01$, and *** $p < 0.001$) and # indicates statistically significant differences compared to 3D Ctrl (# $p < 0.05$ and ### $p < 0.001$).

a slight enhancement in its activity, were exhibited after 3 days in both cell models. Prior research pointed out the requirement of FASN upregulation for CSC maintenance.[21] Dianat-Moghadam et al demonstrated that FASN, together with other metabolic enzymes, regulates CSC clonogenicity in colon cancer.[28] Specifically, higher levels of fatty acids are implicated in the activating signaling pathways crucial for CSC proliferation.[22] Thus, these findings suggest that the upregulation of FASN facilitates the expansion and proliferation of LCSCs in this particular 3D culture environment.

Subsequently, EGFR and its downstream signaling pathways (AKT, MAPK, and STAT3) were analyzed in LCSCs cultured in PCL-ES scaffolds (Figure 2). A decrease in both phosphorylated and total EGFR levels was revealed in both cell models. These findings align with our previous research, in which triple-negative breast cancer (TNBC) cells cultured in poly(lactic acid) (PLA)-ES scaffolds also showed reduced p-EGFR expression.[29] In addition, Ekert et al demonstrated a decrease in total EGFR levels in various lung adenocarcinoma cell lines, including those harboring EGFR mutations, when cultured in 3D conditions.[30] Collectively, our results suggest that 3D cell culture led to a downregulation of EGFR. Nonetheless, distinct behaviors in the downstream signaling pathways were displayed for each cell model.

Regarding the sensitive model, PC9 cells displayed activation of AKT, MAPK, and STAT3 despite the observed decrease in EGFR. Arasada et al proved that blocking EGFR led to activation of the Notch signaling pathway, resulting in an increase in CSCs.[31] It has been reported that the non-canonical Notch pathway modulates both the JAK/STAT and

PI3K/AKT signaling pathways.[32] Additionally, Zhou et al described that the MAPK pathway was reactivated following EGFR blockade in EGFR-amplified esophageal squamous cell carcinoma.[33] Based on these findings, we hypothesize that the reduction in EGFR levels observed in PC9 cells cultured on PCL-ES scaffolds triggered (I) Notch pathway activation, which in turn, resulted in enhanced levels of p-STAT3 and p-AKT, and (II) MAPK activation (Figure 6A).

Regarding the EGFR-TKI-resistant model, no changes were visualized in p-STAT3 levels. One of the resistance mechanisms of PC9-GR3 cells is the overexpression of Axl.[34] The JAK/STAT pathway is a downstream effector of the Axl receptor.[35,36] Hence, our results suggest EGFR-independent regulation of the JAK/STAT pathway in PC9-GR3 cells, being Axl signaling the main driver of STAT3 activation in PC9-GR3. Furthermore, 3D-cultured PC9-GR3 cells exhibited a decrease in p-MAPK and p-AKT levels, followed by AKT reactivation after 6 days. Our research group demonstrated that 3D cell culture induced MAPK downregulation in TNBC cells, resulting in a quiescent cell profile.[12] We and others observed that FASN inhibition resulted in AKT inactivation,[20,37,38] indicating that FASN influences PI3K/AKT signaling pathway. Based on this evidence, we hypothesize that the overexpression and overactivation of FASN is responsible for AKT reactivation in 3D-cultured PC9-GR3 cells (Figure 6C).

Afterwards, the second objective of our study was addressed: evaluating the cytotoxic effect of G28 against LCSCs (Figure 3). Our data revealed that G28 treatment exhibited a cytotoxic effect in both 2D- and 3D-cultured cells. Concretely, PC9-LCSCs were equally sensitive to G28 treatment as 2D-cultured cells, while PC9-GR3-LCSCs exhibited resistance. The IC_{50} value of 3D-cultured PC9-GR3 cells was twice as high as in monolayer conditions, though this difference lacked statistical significance.

Ali et al described that resistant EGFRm NSCLC cells showed palmitoylated EGFR in both the membrane and the nucleus, promoting FASN expression as resistance strategy.[19] However, in 2D conditions, the IC_{50} value of PC9 cells was 1.7-fold higher than PC9-GR3. These findings might be attributed to a potential off-target effect of G28 on Bcl-2, an anti-apoptotic protein overexpressed in PC9-GR3 cells,[34] since Olotu et al demonstrated that EGCG inhibited Bcl-2.[39] Thus, G28 might exhibit a dual cytotoxic effect: inhibiting FASN activity and targeting Bcl-2. Interestingly, cell viability was similar between 2D and 3D cultures after G28 treatment for both cell models, except at the 30 μM dose. These findings differ from those reported with osimertinib treatment, in which 3D-cultured cells exhibited significantly higher resistance compared to monolayer-cultured cells.[13] Additionally, G28 treatment reduced FASN protein levels in both sensitive and EGFR-TKI-resistant cell models, which leads to decreased cell proliferation in NSCLC cells.[38] Similar observations were reported by Tan et al after the treatment with galloyl ester-containing compounds, such as G28.[40]

Afterwards, the molecular effects of G28 treatment on LCSC biomarkers and EGFR and its downstream signaling pathways (AKT, MAPK, and STAT3) were investigated in 2D- and 3D-cultured cells (Figures 4 and 5). The SREBP-1/FASN lipogenic signaling pathway has been identified as essential for LCSCs in NSCLC, as blocking FASN reduces stemness (36), migration, invasion, and colony formation capacities (33,37).

Regarding PC9 cells, increased CD166 and p-SOX2 levels, along with decreased E-cadherin expression indicated an expansion of LCSCs. G28 treatment reduced CD166 and p-SOX2 levels to those observed in 2D-cultured cells, while not altering E-cadherin expression. Additionally, G28 treatment resulted in an increase in total EGFR protein levels, and a decrease in p-STAT3, p-AKT, and total AKT levels. Interestingly, CD166 and SOX2 expression are regulated by the AKT signaling pathway,[41,42] while E-cadherin is controlled by the MAPK pathway.[43] It has been reported that FASN inhibition downregulated both AKT and MAPK signaling pathways in NSCLC,[38] differing from our results. Hence, this supports our hypothesis that MAPK signaling pathway is regulated differently than the AKT and STAT3 pathways in PC9-LCSCs, since G28 treatment affected AKT/CD166-SOX2 and STAT3, but not MAPK/E-Cadherin.

Regarding PC9-GR3 cells, no changes were showed in LCSCs markers in 3D-cultured cells, except for a slight decrease in E-cadherin expression, since this cell model requires a longer period in 3D environment to observe changes in various LCSC markers.[13] In fact, an increase in p-AKT levels was visualized after 6 days of culture (Figure 2), which is associated with LCSC niche.[44,45] Yang et al demonstrated that FASN inhibition using cerulenin significantly reduced epidermal-mesenchymal transition (EMT) in cisplatin-resistant cells.[46] Nevertheless, our data revealed no variations in LCSC markers after G28 treatment. Additionally, the treatment increased EGFR activation, but reduced p-AKT and p-MAPK levels, indicating a direct link between FASN levels and AKT activation, in agreement with a previous study.[38] No alterations were observed in STAT3. These results support the hypothesis that (I) the JAK/STAT pathway is regulated

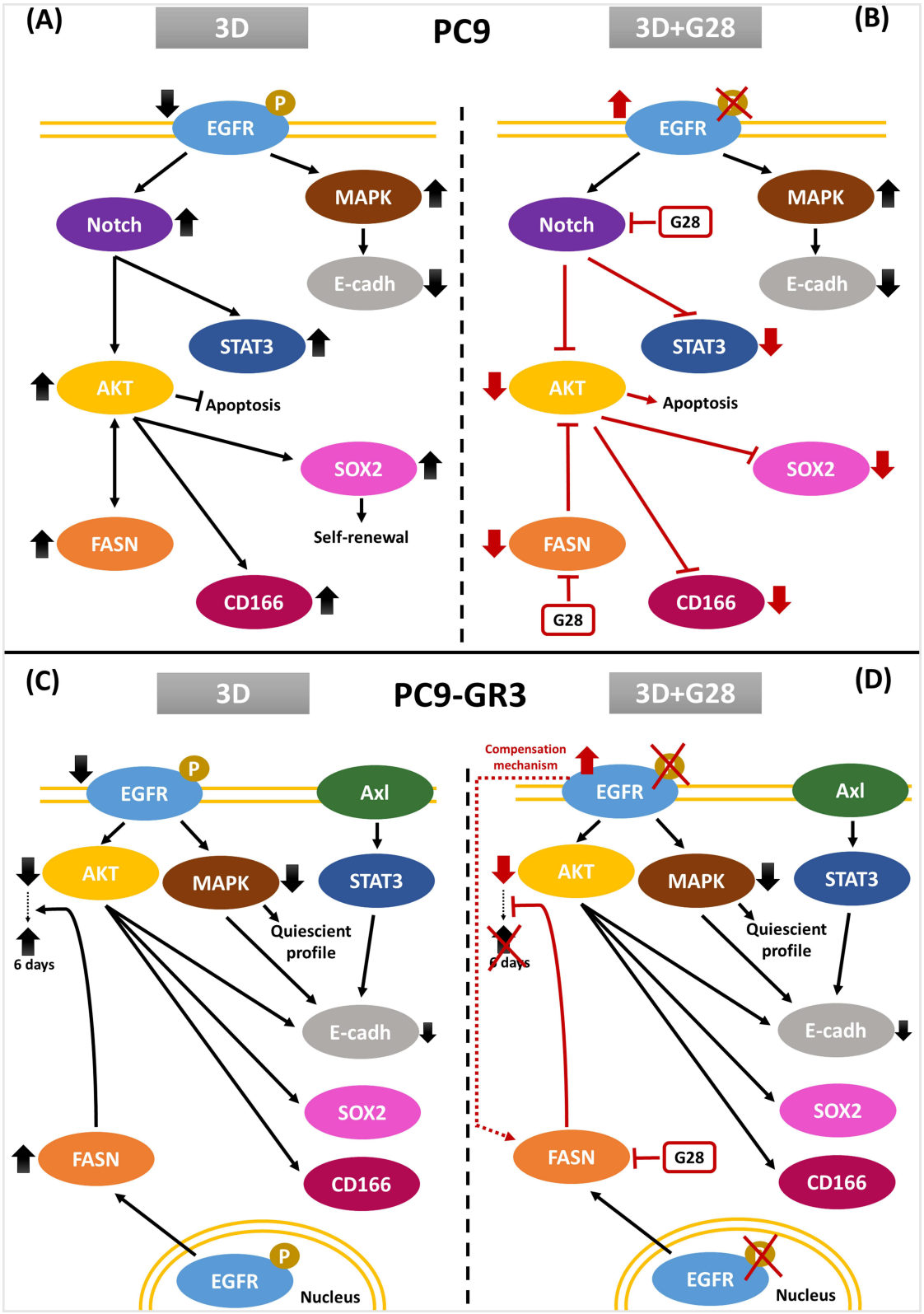

Figure 6 Overview of (I) the role of FASN, EGFR and their downstream signaling pathways in PC9 (**A**) and PC9-GR3 (**C**) cells cultured in PCL-ES scaffolds and (II) the mechanism of action of compound G28 in PC9 (**B**) and PC9-GR3 (**D**) cells cultured in PCL-ES scaffolds.
Abbreviations: EGFR, Epidermal Growth Factor Receptor; P, palmitate group; MAPK, Mitogen-Activated Protein Kinase; AKT, Protein Kinase B; STAT3, Signal Transducer and Activator of Transcription 3; E-cadh, E-cadherin; SOX2, SRY-Box Transcription Factor 2; CD166, Cluster of Differentiation 166; FASN, Fatty Acid Synthase.

https://doi.org/10.2147/LCTT.S512936

by Axl, being independent of EGFR, in the resistant model[34–36] and (II) the overexpression and overactivation of FASN is responsible for AKT reactivation in 3D-cultured PC9-GR3 cells after 6 days.[20,37,38]

Considering all the evidence, it is hypothesized that the compound G28 has different mechanisms of action depending on the cell model. In the sensitive model, two potential mechanisms of action for G28 are suggested. The first mechanism is that G28 inhibits both FASN activity[18] and protein expression, potentially leading to AKT inhibition. Consequently, it may have multiple effects: (I) suppression of STAT3 activation due to cross-talk between the two pathways;[47] (II) downregulation of CD166 and SOX2, resulting in a reduced LCSC population; and (III) activation of apoptosis.[18,40] The second mechanism is that G28 may have off-target effect on Notch since several researchers have reported that EGCG inhibited the Notch signaling pathway.[48,49] Thus, Notch inhibition potentially leads to the suppression of STAT3 and AKT/CD166-SOX2 pathways.[32] The absence of changes in the MAPK pathway suggests that the observed increase in EGFR expression might be a compensatory response by the cells to the treatment, rather than a direct effect of G28 (Figure 6B). In contrast, in the resistant model, the potential mechanism of action is that G28 inhibits both the activity[18] and expression of FASN, thereby possibly preventing AKT activation. As a result, it is hypothesized that LCSC expansion is inhibited since this signaling pathway plays an important role in the regulation of this malignant population.[41,42] In contrast to PC9 cells, EGFR activation in PC9-GR3-LCSCs is proposed to contribute to their resistance to G28 treatment, since EGFRm directly upregulates FASN expression.[18,19] These findings suggest the theory that a G28 monotherapy may be effective in sensitive cells, whereas a combinatorial treatment of G28 with EGFR-TKIs may be required in resistant cells to effectively inhibit the expansion of LCSC niche. In fact, our research group demonstrated that G28 treatment re-sensitizes PC9-GR3 cells to osimertinib and gefitinib (Figure 6D).[18] However, further experiments are necessary to confirm these hypotheses.

While the findings offer valuable insights into the role of FASN and the impact of G28 treatment, several limitations should be acknowledged. First, the exclusive use of PCL-ES scaffolds may not adequately replicate the complexity of the tumor microenvironment. Second, the relatively short culture duration may fail to capture long-term effects, particularly in EGFR-TKI-resistant cells. Third, the study was limited to two EGFRm NSCLC cell lines, which constrains the generalizability of the results. Fourth, all assays were conducted in vitro, so the results may not directly translate to in vivo settings. Finally, potential off-target effects of G28 and the limited assessment of its efficacy in combination with other therapeutic agents require further investigation.

Conclusions

FASN plays a critical role in the proliferation and maintenance of LCSCs cultured in PCL-ES scaffolds. The enzyme was upregulated in both sensitive and EGFR-TKI-resistant EGFRm NSCLC cells cultured in 3D conditions suggesting its potential relevance in this malignant subpopulation. In addition, the treatment with G28, a synthetic derivative of EGCG, exhibited cytotoxic effects in both cell models. Specifically, FASN inhibition resulted in the downregulation of AKT, which is crucial for the survival and expansion of the LCSC niche. Finally, our findings suggest that a therapeutic strategy combining G28 and EGFR-TKIs could re-sensitize EGFR-TKI-resistant cells and eradicate LCSCs. However, further experiments are needed to explore its clinical feasibility. Therefore, FASN inhibition using G28 emerges as a promising therapeutic approach against LCSCs in EGFRm NSCLC cells.

Abbreviations

2D, two dimensional; 3D, three dimensional; AKT, protein kinase B; CD166, cluster of differentiation 166; CSCs, cancer stem cells; EGCG, (−)-epigallocatechin-3-gallate; EGFR, epidermal growth factor receptor; EGFRm, epidermal growth factor receptor mutated; EGFR-TKIs, epidermal growth factor receptor tyrosine kinase inhibitors; EMT, epidermal-mesenchymal transition; FASN, fatty acid synthase; FFA, free fatty acid; JAK, janus kinase; LCSCs, lung cancer stem cells; MAPK, mitogen-activated protein kinase; MTT, 3-(4,5–dimethyl-2–thiazolyl)-2,5–diphenyl-2 H-tetrazolium bromide; NSCLC, non-small cell lung cancer; PCL-ES, polycaprolactone electrospun; PI3K, phosphoinositide 3-kinase;

SOX2, SRY-box transcription factor 2; SREBP-1, sterol regulatory element-binding protein 1; STAT3, signal transducer and activator of transcription 3.

Ethics Approval and Consent to Participate

The use of the cell lines was approved by the Ethics Committee for Investigation with Medicinal Products (CEIm) Girona on February 26, 2019 for protocol code 2019.030.

Acknowledgments

The authors thank the support of Catalan Government (2021SGR01589) and Oncolliga Foundation and RadikalSwim (OncoSwim). The authors are grateful to R. Rosell and M. A. Molina from the laboratory of Oncology Pangaea (Barcelona, Spain) for kindly providing PC9 and PC9-GR3 models.

Author Contributions

All authors made a significant contribution to the work reported, whether that is in the conception, study design, execution, acquisition of data, analysis and interpretation, or in all these areas; took part in drafting, revising or critically reviewing the article; gave final approval of the version to be published; have agreed on the journal to which the article has been submitted; and agree to be accountable for all aspects of the work.

Funding

This work was funded by Spanish grant from Instituto de Salud Carlos III and co-funded by European Union ERDF/ESF, "A way to make Europe"/ "Investing in your future")(PI19/00372). It was also supported by PLEC2021-007523 / AEI / 10.13039/501100011033 and by the European Union –NextGenerationEU. The authors acknowledge the pre-doctoral grants of S.A.-B. (2024FI-100866) and G.R.-L. (IFUdG2020).

Disclosure

The authors declare no conflicts of interest in this work.

References

1. International agency for research on cancer cancer today Available from: https://gco.iarc.fr/today/en. Accessed February 17, 2024.
2. Zhang YL, Yuan JQ, Wang KF, et al. The prevalence of EGFR mutation in patients with non-small cell lung cancer: a systematic review and meta-analysis. *Oncotarget*. 2016;7(48):78985. doi:10.18632/ONCOTARGET.12587
3. Li AR, Chitale D, Riely GJ, et al. EGFR mutations in lung adenocarcinomas: clinical testing experience and relationship to EGFR gene copy number and immunohistochemical expression. *J Mol Diagn*. 2008;10(3):242–248. doi:10.2353/jmoldx.2008.070178
4. Cohen MH, Williams GA, Sridhara R, Chen G, Pazdur R. FDA drug approval summary: gefitinib (ZD1839) (Iressa®) tablets. *Oncologist*. 2003;8(4):303–306. doi:10.1634/theoncologist.8-4-303
5. Greig SL. Osimertinib: first global approval. *Drugs*. 2016;76:263–273. doi:10.1007/S40265-015-0533-4
6. Kobayashi S, Boggon TJ, Dayaram T, et al. EGFR mutation and resistance of non–small-cell lung cancer to gefitinib. *N Engl J Med*. 2005;352(8):786–792. doi:10.1056/NEJMOA044238
7. Thress KS, Paweletz CP, Felip E, et al. Acquired EGFR C797S mutation mediates resistance to AZD9291 in non–small cell lung cancer harboring EGFR T790M. *Nature Med*. 2015;21(6):560–562. doi:10.1038/nm.3854
8. Sun R, Hou Z, Zhang Y, Jiang B. Drug resistance mechanisms and progress in the treatment of EGFR-mutated lung adenocarcinoma (Review). *Oncol Lett*. 2022;24(5). doi:10.3892/ol.2022.13528
9. Rowbotham SP, Goruganthu MUL, Arasada RR, Wang WZ, Carbone DP, Kim CF. Lung cancer stem cells and their clinical implications. *Cold Spring Harb Perspect Med*. 2022;12. doi:10.1101/CSHPERSPECT.A041270
10. Kapałczyńska M, Kolenda T, Przybyła W, et al. 2D and 3D cell cultures – a comparison of different types of cancer cell cultures. *Arch Med Sci*. 2018;14(4):910. doi:10.5114/AOMS.2016.63743
11. Rabionet M, Yeste M, Puig T, Ciurana J. Electrospinning PCL scaffolds manufacture for three-dimensional breast cancer cell culture. *Polymers*. 2017;9(8):328. doi:10.3390/polym9080328
12. Rabionet M, Polonio-Alcalá E, Relat J, et al. Fatty acid synthase as a feasible biomarker for triple negative breast cancer stem cell subpopulation cultured on electrospun scaffolds. *Mater Today Bio*. 2021;12:100155. doi:10.1016/j.mtbio.2021.100155
13. Polonio-Alcalá E, Rabionet M, Ruiz-Martínez S, et al. Polycaprolactone electrospun scaffolds produce an enrichment of lung cancer stem cells in sensitive and resistant EGFRm lung adenocarcinoma. *Cancers*. 2021;13(21):5320. doi:10.3390/cancers13215320
14. Reneker DH, Chun I. Nanometre diameter fibres of polymer, produced by electrospinning. *Nanotechnology*. 1996;7(3):216–223. doi:10.1088/0957-4484/7/3/009

15. Cipitria A, Skelton A, Dargaville TR, Dalton PD, Hutmacher DW. Design, fabrication and characterization of PCL electrospun scaffolds - a review. *J Mater Chem*. 2011;21(26):9419–9453. doi:10.1039/c0jm04502k
16. Hanahan D. Hallmarks of cancer: new dimensions. *Cancer Discov*. 2022;12(1):31–46. doi:10.1158/2159-8290.CD-21-1059
17. Xiao Y, Yang Y, Xiong H, Dong G. The implications of FASN in immune cell biology and related diseases. *Cell Death Dis*. 2024;15(1). doi:10.1038/S41419-024-06463-6
18. Polonio-Alcalá E, Palomeras S, Torres-Oteros D, et al. Fatty acid synthase inhibitor G28 shows anticancer activity in EGFR tyrosine kinase inhibitor resistant lung adenocarcinoma models. *Cancers*. 2020;12(5):1–18. doi:10.3390/cancers12051283
19. Ali A, Levantini E, Teo JT, et al. Fatty acid synthase mediates EGFR palmitoylation in EGFR mutated non-small cell lung cancer. *EMBO Mol Med*. 2018;10(3):1–19. doi:10.15252/emmm.201708313
20. Polonio-Alcalá E, Porta R, Ruiz-Martínez S, et al. AZ12756122, a novel fatty acid synthase inhibitor, decreases resistance features in EGFR-TKI resistant EGFR-mutated NSCLC cell models. *Biomed Pharmacother*. 2022;156:113942. doi:10.1016/j.biopha.2022.113942
21. Castagnoli L, Corso S, Franceschini A, et al. Fatty acid synthase as a new therapeutic target for HER2-positive gastric cancer. *Cell Oncol*. 2023;46 (3):661–676. doi:10.1007/S13402-023-00769-X
22. Wang X, Xiao J, Xiao J, et al. Cholesterol and saturated fatty acids synergistically promote the malignant progression of prostate cancer. *Neoplasia*. 2022;24(2):86–97. doi:10.1016/J.NEO.2021.11.004
23. Capasso L, De Masi L, Sirignano C, et al. Epigallocatechin gallate (EGCG): pharmacological properties, biological activities and therapeutic potential. *Molecules*. 2025;30(3):654. doi:10.3390/MOLECULES30030654
24. Li D, Cao D, Sun Y, et al. The roles of epigallocatechin gallate in the tumor microenvironment, metabolic reprogramming, and immunotherapy. *Front Immunol*. 2024;15. doi:10.3389/FIMMU.2024.1331641
25. Puig T, Aguilar H, Cufí S, et al. A novel inhibitor of fatty acid synthase shows activity against HER2+ breast cancer xenografts and is active in Anti-HER2 drug-resistant cell lines. *Breast Cancer Res*. 2011;13(6). doi:10.1186/BCR3077
26. Giró-Perafita A, Rabionet M, Planas M, et al. EGCG-derivative G28 shows high efficacy inhibiting the mammosphere-forming capacity of sensitive and resistant TNBC models. *Molecules*. 2019;24(6):1–15. doi:10.3390/molecules24061027
27. Polonio-Alcalá E, Rabionet M, Guerra A, Yeste M, Ciurana J, Puig T. Screening of additive manufactured scaffolds designs for triple negative breast cancer 3d cell culture and stem-like expansion. *Int J Mol Sci*. 2018;19(10):3148. doi:10.3390/ijms19103148
28. Dianat-Moghadam H, Khalili M, Keshavarz M, et al. Modulation of LXR signaling altered the dynamic activity of human colon adenocarcinoma cancer stem cells in vitro. *Cancer Cell Int*. 2021;21(1). doi:10.1186/S12935-021-01803-4
29. Polonio-Alcalá E, Rabionet M, Gallardo X, et al. PLA electrospun scaffolds for three-dimensional triple-negative breast cancer cell culture. *Polymers*. 2019;11(5):916. doi:10.3390/polym11050916
30. Ekert JE, Johnson K, Strake B, et al. Three-dimensional lung tumor microenvironment modulates therapeutic compound responsiveness in vitro--implication for drug development. *PLoS One*. 2014;9(3):e92248. doi:10.1371/JOURNAL.PONE.0092248
31. Arasada RR, Amann JM, Rahman MA, Huppert SS, Carbone DP. EGFR blockade enriches for lung cancer stem-like cells through Notch3-dependent signaling. *Cancer Res*. 2014;74(19):5572–5584. doi:10.1158/0008-5472.CAN-13-3724
32. Shi Q, Xue C, Zeng Y, et al. Notch signaling pathway in cancer: from mechanistic insights to targeted therapies. *Signal Transduct Target Ther*. 2024;9(1):128. doi:10.1038/s41392-024-01828-x
33. Zhou J, Wu Z, Wong G, et al. CDK4/6 or MAPK blockade enhances efficacy of EGFR inhibition in oesophageal squamous cell carcinoma. *Nat Commun*. 2017;8. doi:10.1038/ncomms13897
34. Jacobsen K, Bertran-Alamillo J, Molina MA, et al. Convergent Akt activation drives acquired EGFR inhibitor resistance in lung cancer. *Nat Commun*. 2017;8(1). doi:10.1038/s41467-017-00450-6
35. Tanaka M, Siemann DW. Therapeutic targeting of the Gas6/Axl signaling pathway in cancer. *Int J Mol Sci*. 2021;22(18):9953. doi:10.3390/ijms22189953
36. Hung CN, Chen M, DeArmond DT, et al. AXL-initiated paracrine activation of PSTAT3 enhances mesenchymal and vasculogenic supportive features of tumor-associated macrophages. *Cell Rep*. 2023;42(9):113067. doi:10.1016/J.CELREP.2023.113067
37. Ventura R, Mordec K, Waszczuk J, et al. Inhibition of de novo palmitate synthesis by fatty acid synthase induces apoptosis in tumor cells by remodeling cell membranes, inhibiting signaling pathways, and reprogramming gene expression. *EBioMedicine*. 2015;2(8):808. doi:10.1016/J.EBIOM.2015.06.020
38. Chang L, Fang S, Chen Y, et al. Inhibition of FASN suppresses the malignant biological behavior of non-small cell lung cancer cells via deregulating glucose metabolism and AKT/ERK pathway. *Lipids Health Dis*. 2019;18(1):118. doi:10.1186/S12944-019-1058-8
39. Olotu FA, Agoni C, Adeniji E, Abdullahi M, Soliman ME. Probing gallate-mediated selectivity and high-affinity binding of epigallocatechin gallate: a way-forward in the design of selective inhibitors for anti-apoptotic Bcl-2 proteins. *Appl Biochem Biotechnol*. 2019;187(3):1061–1080. doi:10.1007/S12010-018-2863-7
40. Tan Y-J, Ali A, Tee S-Y, et al. Galloyl esters of trans-stilbenes are inhibitors of FASN with anticancer activity on non-small cell lung cancer cells. *Eur J Med Chem*. 2019;182:111597. doi:10.1016/j.ejmech.2019.111597
41. Zhang S, Xiong X, Sun Y. Functional characterization of SOX2 as an anticancer target. *Signal Transduction Targeted Ther*. 2020;5(1):1–17. doi:10.1038/s41392-020-00242-3
42. Ma L, Wang J, Lin J, Pan Q, Yu Y, Sun F. Cluster of differentiation 166 (CD166) regulated by phosphatidylinositide 3-kinase (PI3K)/AKT signaling to exert its anti-apoptotic role via yes-associated protein (YAP) in liver cancer. *J Biol Chem*. 2014;289(10):6921–6933. doi:10.1074/JBC.M113.524819
43. Loh CY, Chai JY, Tang TF, et al. The E-cadherin and N-cadherin switch in epithelial-to-mesenchymal transition: signaling, therapeutic implications, and challenges. *Cells*. 2019;8(10):1118. doi:10.3390/CELLS8101118
44. Moghbeli M. PI3K/AKT pathway as a pivotal regulator of epithelial-mesenchymal transition in lung tumor cells. *Cancer Cell Int*. 2024;24:1–13. doi:10.1186/S12935-024-03357-7
45. Kim IG, Lee JH, Kim SY, Heo CK, Kim RK, Cho EW. Targeting therapy-resistant lung cancer stem cells via disruption of the AKT/TSPYL5/PTEN positive-feedback loop. *Commun Biol*. 2021;4:1–17. doi:10.1038/s42003-021-02303-x
46. Yang L, Zhang F, Wang X, et al. A FASN-TGF-B1-FASN regulatory loop contributes to high EMT/ metastatic potential of cisplatin-resistant non-small cell lung cancer. *Oncotarget*. 2016;7(34):55543–55554. doi:10.18632/oncotarget.10837

47. Sun Z, Jiang Q, Gao B, et al. AKT blocks SIK1-mediated repression of STAT3 to promote breast tumorigenesis. *Cancer Res*. 2023;83 (8):1264–1279. doi:10.1158/0008-5472.CAN-22-3407
48. Wei H, Ge Q, Zhang LY, et al. EGCG inhibits growth of tumoral lesions on lip and tongue of K-Ras transgenic mice through the notch pathway. *J Nutr Biochem*. 2022;99:108843. doi:10.1016/J.JNUTBIO.2021.108843
49. Wang YN, Wang J, Yang HN, et al. The oxidation of (−)-epigallocatechin-3-gallate inhibits T-cell acute lymphoblastic leukemia cell line HPB-ALL via the regulation of Notch1 expression. *RSC Adv*. 2020;10(3):1679–1684. doi:10.1039/C9RA08459B